water

MDPI

Article

Modeling and Optimization of Electrochemical Advanced Oxidation of Clopidogrel Using the Doehlert Experimental Design Combined with an Improved Grey Wolf Algorithm

Dorsaf Mansour [1,*], Eman Alblawi [1], Abdulmohsen Khalaf Dhahi Alsukaibi [1], Jamal Humaidi [1], Hichem Tahraoui [2,3,4], Manar Shatat [1], Safa Teka [1], Sawsan Maisara [1], Nizar Bellakhal [5], Housam Binous [6] and Abdeltif Amrane [4]

1 Chemistry Department, College of Sciences, University of Ha'il, P.O. Box 2440, Ha'il 81451, Saudi Arabia
2 Laboratoire de Génie des Procédés Chimiques, Department of Process Engineering, University of Ferhat Abbas, Setif 19000, Algeria; hichemm.tahraouii@gmail.com
3 Laboratory of Biomaterials and Transport Phenomena (LBMPT), Nouveau Pôle Urbain, Medea University, Medea 26000, Algeria
4 Ecole Nationale Supérieure de Chimie de Rennes, Université de Rennes 1, CNRS, UMR 6226, 11 Allée de Beaulieu, CS 50837, 35708 Rennes CEDEX 7, France; abdeltif.amrane@univ-rennes1.fr
5 Laboratory of Eco-Chimie, National Institute of Applied Sciences & Technology, P.O. Box 676, Tunis 1080, Tunisia
6 Chemical Engineering Department, National Institute of Applied Sciences & Technology, P.O. Box 676, Tunis 1080, Tunisia
* Correspondence: d.mansour@uoh.edu.sa; Tel.: +966-551506526

Abstract: In this research, the optimization of the electrochemical advanced oxidation treatment for the degradation of Clopidogrel was investigated. This study examined the influence of various experimental parameters including applied current, initial Clopidogrel concentration, and ferrous ion concentration by the use of the Doehlert design within a response surface methodology framework. The improved grey wolf optimizer was applied in order to define the optimum operating conditions. The monitoring of clopidogrel concentration during treatment revealed that complete disappearance of clopidogrel was achieved under an initial clopidogrel concentration of 0.02 mM, current intensity of 0.55 A, Fe^{2+}concentration of 0.7 mM, and a reaction time of 20 min in a solution containing 50 mM Na_2SO_4 at pH 3. A quadratic polynomial model was developed, and its statistical significance was confirmed through the analysis of variance, demonstrating a high level of confidence in the model (R^2 = 0.98 and p-value < 0.05). Furthermore, following electrolysis treatment for 480 min, the synthetic clopidogrel solutions underwent mineralization, achieving a 70.4% removal rate of total organic carbon. Subsequently, the applicability of the optimized process was tested on real pharmaceutical wastewater, and mineralization was investigated under the identified optimal conditions, resulting in a total organic carbon removal rate of 87% after 480 min of electrolysis time. The energy consumption for this system was calculated to be 1.4 kWh·kg^{-1} of the total organic carbon removed. These findings underscore the effectiveness and potential applicability of the electrochemical advanced oxidation for industrial wastewater treatment.

Keywords: clopidogrel; electrochemical processes; mineralization; improved grey wolf optimizer; Doehlert experimental design

check for updates

Citation: Mansour, D.; Alblawi, E.; Alsukaibi, A.K.D.; Humaidi, J.; Tahraoui, H.; Shatat, M.; Teka, S.; Maisara, S.; Bellakhal, N.; Binous, H.; et al. Modeling and Optimization of Electrochemical Advanced Oxidation of Clopidogrel Using the Doehlert Experimental Design Combined with an Improved Grey Wolf Algorithm. *Water* **2024**, *16*, 1964. https://doi.org/10.3390/w16141964

Academic Editor: Sergi Garcia-Segura

Received: 7 June 2024
Revised: 1 July 2024
Accepted: 5 July 2024
Published: 11 July 2024

Copyright: © 2024 by the authors. Licensee MDPI, Basel, Switzerland. This article is an open access article distributed under the terms and conditions of the Creative Commons Attribution (CC BY) license (https://creativecommons.org/licenses/by/4.0/).

1. Introduction

Pharmaceuticals are chemical substances with biological activity and a specific purpose of action [1]. Indeed, by harnessing their biological activity, these medicines work to cure diseases, defeat infections, and bring relief from symptoms [2]. Several environmental compartments, particularly aquatic ecosystems, have shown evidence of pharmaceutical contamination, solidifying their classification as emerging pollutants [3–6]. Most of these

substances are derived from industries, homes, clinics, and hospitals, and their release into the environment poses a potential threat to both aquatic life and human health [7]. Trace amounts of pharmaceutical compounds, ranging from ng·L^{-1} to µg·L^{-1}, have been detected in aquatic environments globally [8]. According to a World Health Organization (WHO) report in 2012, pharmaceutical concentrations are typically below 0.1 µg L^{-1}, with treated water generally having concentrations less than 0.05 µg L^{-1} [9].

The widespread presence of pharmaceutical residues in the environment poses a significant threat, as they can cause significant health problems and even death in living organisms [10]. Indeed, these toxic pollutants can contaminate water supplies, leading to a range of health problems like kidney disease, skin and eye irritation, respiratory issues, and heart troubles [8]. Some substances exhibit mutagenic and carcinogenic properties, which indicate their potential to cause tumor formation and genetic abnormalities [11]; others pose a significant threat to vultures, higher plants, aquatic organisms, and mammals, raising serious health concerns and threats [12]. Consequently, the urgent need to protect the environment necessitates the development of efficacious methods for the removal of pharmaceutical residues from wastewater.

Several analytical techniques have been employed to determine pharmaceuticals in diverse water samples, including the enzyme-linked immunosorbent assay (ELISA), which is a traditional technique used for detecting pharmaceutical residues in meat, milk, surface water, groundwater, wastewater, soil, and manure [13]. Moreover, chromatographic techniques have been widely applied for the analysis of pharmaceuticals, notably, high-performance liquid chromatography–ultraviolet detection (HPLC-UV), high-performance liquid chromatography–diode array detection (HPLC-DAD), liquid chromatography–mass spectrometry (LC-MS), liquid chromatography–mass spectrometry/mass spectrometry (LC-MS/MS), and gas chromatography-mass spectrometry (GC-MS) [14].

Conventional sewage treatment methods are not designed to remove pharmaceutical substances effectively [15–17]. As a result, more than 90% of these compounds survive the treatment process and end up accumulating in domestic and sewage waste [15].

Driven by concerns about the detrimental effects of pharmaceutical compounds, researchers have persistently pursued methods to eliminate them from the environment. Several techniques such as coagulation/flocculation, adsorption, biodegradation, incineration, chlorination, and reverse osmosis have been assessed for this purpose [18–21]. Though these methods are effective in removing recalcitrant compounds, their main downside is the transfer of pollutants from one phase to another, resulting in the production of secondary waste that cannot be treated again and dumped as such [22]. Hence, the development of an efficient method for eliminating pharmaceutical substances is necessary.

Advanced oxidation processes (AOPs) are potentially effective methods for wastewater treatment, especially when contaminant species are resistant to biological processes [23]. These processes rely on generating powerful oxidants, particularly hydroxyl radicals (•OH), and involve Fenton's reagent, peroxonation, homogeneous photocatalysis (Fe^{3+}/UV), heterogeneous photocatalysis (TiO_2/UV), H_2O_2/ozonation processes, sonochemical process, anodic oxidation, and electro-Fenton processes [24–30].

Electro-Fenton is an electrochemical advanced oxidation process that uses the Fenton reaction to produce hydroxyl radicals. In the electro-Fenton reaction, a mixture of H_2O_2 and Fe^{2+} is generated electrochemically throughout the process [31–35]. Indeed, H_2O_2 is produced by the reduction of the added O_2 at the cathode. This later reacts with the introduced Fe^{2+} ions, in an acidic medium, to generate the hydroxyl radicals [36–38]. Because of its high oxidation potential, •OH exhibits exceptional reactivity, enabling the rapid hydroxylation or dehydration of a vast range of organic pollutants to produce inorganic ions, carbon dioxide (CO_2), and water [23,39,40].

Clopidogrel bisulfate ($C_{16}H_{18}ClNO_6S_2$) is a thienopyridine that is 4,5,6,7-tetrahydrothie no[3,2-c] pyridine, where the hydrogen attached to the nitrogen is substituted with an o-chlorobenzyl group, the methylene hydrogen of which is substituted with a methoxycarbonyl group. This drug acts as an antiplatelet agent employed in the prophylaxis

of blood clot formation, myocardial infarction, stroke, peripheral arterial disease, acute coronary syndrome, and cardiovascular death, and it is marketed under the trade name Plavix® [41,42]. It is widely prescribed and is ranked as the second-highest-selling drug worldwide [42]. However, the ubiquity of this pharmaceutical in municipal and industrial wastewater effluents necessitates its classification as an emerging contaminant [42]. The recurrent identification of this pharmaceutical in water sources can be attributed to the human body's restricted capacity for metabolism, resulting in its subsequent elimination via the urinary system. In addition, industrial activities are considered to be a major contributor to the regular presence of this drug in wastewater because of the discharge of residual compounds [42].

This work investigates three main objectives. The first one is the determination of the optimum experimental conditions for the degradation of clopidogrel in synthetic solution using the Doehlert methodology design combined with the improved grey wolf optimizer, a powerful algorithm that leverages its efficiency and effectiveness to identify optimal process conditions. The Doehlert design is a second-degree polynomial model that efficiently investigates multiple factors at various levels simultaneously. This quadratic model offers a powerful and convenient approach, it transcends traditional procedures that only consider one factor at a time, and allows the exploration of the effects of multiple factors simultaneously, revealing their individual and combined impacts [43]. To fulfill this objective, high-performance liquid chromatography was employed to quantify and track changes in clopidogrel concentration over time. The second objective is to assess clopidogrel mineralization through total organic carbon removal. The final objective is to validate the applicability of the process through its effectiveness in remediating real industrial wastewater. On the whole, this work makes a significant contribution to sustainable wastewater management practices that can reduce organic pollutant releases into the environment.

2. Materials and Methods

2.1. Chemicals

Clopidogrel bisulfate (CPG, purity 98%) was provided by Sigma Aldrich (Saint Quentin Fallavier, France). $FeSO_4.7H_2O$ (purity 99%) and Na_2SO_4 (purity 99%) respectively employed as a reactant and electrolyte support were supplied by Acros Organics (Thermo Fisher Scientific, Illkirch, France). Acetonitrile (purity 99.9%) of HPLC grade was purchased from Sigma Aldrich. Hydrochloric acid from Acros Organics was used to adjust the pH of the CPG solutions. The preparation of all solutions utilized deionized water. All other chemicals employed throughout this study were acquired from Acros Organics and Sigma Aldrich.

2.2. Pharmaceutical Effluent

For this study, the effluent originated from a pharmaceutical manufacturing facility situated in Hail City in Saudi Arabia. The sample was carefully collected and sealed in a container. With a view to ensure its integrity, it was stored under optimal conditions: protected from light and maintained at a constant temperature of 4 °C.

2.3. Analytical Determinations

Prior to further analysis, the solutions were filtered using Sartorius Minisart® 0.45 µm GF prefilters (Goettingen, Germany).

CPG removal was tracked by HPLC using the UltiMate 3000 System equipped with UltiMate 3000 PDA (Photodiode Array Detector) from Thermo Scientific (Oxford, UK) and a UltiMate 3000 SD Pump from Thermo Scientific (Oxford, UK). The separation was performed on a Waters C18, (5 µm; 4.6 × 250 mm) reversed-phase column. The eluent was prepared by mixing acetonitrile and ultra-pure water in a specific ratio (30/70 v/v) and was delivered through the HPLC system at a constant flow rate of 1 mL min^{-1}. Clopidogrel

detection was performed at a wavelength of 235 nm. The analytical device was controlled by Chromeleon CDS 7.2 software.

The total organic carbon (TOC) content of the solution was examined was prior to and throughout the treatment process using a TOC-$V_{CPH/CPN}$ analyzer from Shimadzu (Wolverton, UK). The organic carbon compounds underwent combustion, resulting in the conversion to CO_2, subsequently detected by a non-dispersive infrared sensor (NDIR). The standard non-purgeable organic carbon (NPOC) was used to achieve reproducible TOC values. Triplicate measurements were performed on each sample to ensure data reliability and reproducibility.

The total nitrogen (TN_b) of the initial sample was determined using a TOC analyzer. The total suspended solids (TSS) was obtained by centrifugation then drying at 105 °C. Nanocolor® tests CSB 4000 purchased from Macherey-Nagel (Düren, Germany) were employed to measure the Chemical Oxygen Demand (COD). The nitrate (NO_3^-), nitrite (NO_2^-), and phosphate (PO_4^{3-}) concentrations were determined using Nitrate 50, Nitrite 2, and total Phosphate 15 Nanocolor® tests, respectively.

2.4. Experimental Procedure

Firstly, the electro-Fenton process was used to treat the CPG synthetic solution prepared in deionized water. Secondly, this treatment was applied to the remediation of real pharmaceutical wastewater obtained directly from an industrial facility.

The treatment of CPG was performed in an undivided 300 mL cylindrical cell outfitted with two electrodes. The anode consisted of double platinum wire (Metrohm, Villebon-sur-Yvette, France) and was placed in the central position to achieve uniform potential distribution throughout the cell. The carbon felt cathode (Le Carbone Lorraine RVG 4000, Mersen, Paris La Défense, France) was positioned against the cell inner wall. Its dimensions were 90 mm × 75 mm, specific area was 0.7 $m^2\ g^{-1}$, thickness was 12 mm, density was 0.088 g cm^{-3}, and carbon yield was 99.9%. A direct current power supply (Metrix, model AX 322) was used in galvanostatic mode to provide electrical power to the electrodes and monitor the amperage. To achieve a pH of 3, hydrochloric acid was added to the CPG solutions.

Immediately before initiating electrolysis, $FeSO_4.7H_2O$ was added as catalyst. The ionic strength was kept constant by introducing Na_2SO_4 (50 mM) into the cell as a supporting electrolyte.

The energy consummation (EC) for the electro-Fenton system was calculated according to Equation (1).

$$EC\left(\frac{KWh}{g}\right) = \frac{(U \times I \times t)}{(TOC_0 - TOC_t)V} \quad (1)$$

where EC is the electrical energy consumption (kWh·g^{-1} $TOC_{removed}$), U is the cell voltage (V), I is the applied current (A), t is the reaction time (h), TOC_0 and TOC_t are the initial and residual concentrations of TOC (mg·L^{-1}), and V is the volume of effluent (L).

2.5. Doehlert Experimental Design

Response surface methodology (RSM) is a valuable statistical technique employed to analyze and optimize complex processes. It excels in modeling the relationships among multiple variables and a desired outcome, making it a powerful tool across diverse fields, such as medicine, engineering, and environmental science [44]. The Doehlert experimental design, a second-order polynomial model, permits the concurrent examination of multiple variables at various levels [45]. This model offers the benefit of a reduced experimental demand, and this characteristic makes it highly suitable for resource-intensive research, minimizing costs associated with expensive materials or lengthy experimental processes [44]. Doehlert matrices are further distinguished by their uniform distribution of experimental points. This even spread throughout the parameter space guarantees a thorough investigation of the factor effects [44].

In this context, an investigation into the influence of operational parameters was conducted utilizing the Doehlert experimental design, including current intensity (U_1), initial Fe^{2+} concentration (U_2), and CPG initial concentration (U_3).

The response (Y) corresponds to the CPG removal rate. The Doehlert matrix consists of N experiments, where $N = K^2 + K + 1$ and K is the number of variables. For K = 3, the matrix involved 13 experiments uniformly distributed across the coded variables space.

Three replicates were performed at the central point (experiments 13–15) in order to obtain an estimate of the experimental error. The conversion of natural variables (U_i) into coded variables (X_i) was performed using Equation (2) [46]:

$$X_i = \left[\frac{U_i - U_{i(0)}}{\Delta U_i}\right]\alpha \quad (2)$$

where $U_{i\,(0)}$ is the value of U_i at the center of the study domain, ΔU_i is the variation step, and α is the maximum coded value of X_i: $X_1 = 1$; $X_2 = 0.866$; $X_3 = 0.816$.

$$U_{i(0)} = \frac{\text{upper limit of } U_i + \text{lower limit of } U_i}{2} \quad (3)$$

$$\Delta U_i = \frac{\text{upper limit of } U_i - \text{lower limit of } U_i}{2} \quad (4)$$

For the Doehlert model, a specific domain was defined for each variable ($0.05 < U_1$ (A) < 0.55; $0.2 < U_2$ (mM) < 1; $0{,}02 < U_3$ (mM) < 0.1), determined following preliminary trials.

The measured outcome associated with the Doehlert matrix design is depicted as a quadratic polynomial model:

$$Y = b_0 + b_1X_1 + b_2X_2 + b_3X_3 + b_{11}{X_1}^2 + b_{22}{X_2}^2 + b_{33}{X_3}^2 + b_{12}X_1X_2 + b_{13}X_1X_3 + b_{23}X_2X_3 \quad (5)$$

where Y is the experimental response, b_0 is a constant of the model, b_i is the estimation of the main effects of factor i, b_{ii} is the estimation of the second-order effects, and b_{ij} is the estimation of the interactions between factor i and factor j. The coefficients were calculated with the least squares method by means of

$$B = (X^T X)^{-1} X^T Y \quad (6)$$

where B is the vector of estimates of the coefficients, X is the model matrix, X^T is the transposed model matrix, and Y is the vector of measured response.

An analysis of variance (ANOVA) was employed to verify the model's statistical significance. The three-dimensional response surface and two-dimensional isoresponse curves were drawn to represent the relationship between response and experimental variables graphically. NEMRODW Software (version 9901, France) [47] was employed in the calculation and processing of data.

2.6. Improved Grey Wolf Optimizer (I-GWO)

The grey wolf optimizer (GWO) is a nature-inspired metaheuristic algorithm that leverages the social hierarchy and hunting behavior of grey wolves. The GWO algorithm mimics the leadership structure of a wolf pack. Three wolves, α, β, and δ, representing the best solutions discovered so far, guide the search by directing the remaining pack (ω wolves) towards promising areas within the search space [48]. The wolf hunting consists of three main steps including encircling, hunting, and attacking prey. In GWO, the wolves (α, β, and δ) guide the remaining pack members (ω wolves) towards favorable locations within the search space, helping them find the best overall solution. However, a potential limitation of GWO is the convergence of the search towards local optima [48]. The reduction in population diversity, caused by the leader-centric search strategy, can limit the exploration of promising but less obvious areas of the search space [48]. In an effort to overcome these limitations, this work introduces an improved grey wolf optimizer (IGWO).

IGWO builds on GWO by incorporating enhancements and refinements to improve its optimization performance. These improvements may include modifications to the search mechanisms, such as the exploration and exploitation strategies employed during the optimization process. By incorporating these enhancements, IGWO strives to achieve superior performance in three key areas including the convergence rate, solution quality, and robustness.

3. Results and Discussion

3.1. Application of the Doehlert Experimental Design

The electro-Fenton method's performance is influenced by various parameters such as current intensity, Fe^{2+}, and CPG initial concentration. With the aim of exploring the effects of these factors simultaneously, the Doehlert matrix was used.

Moreover, the implementation of this approach enabled the development of a mathematical model correlating three input variables (I (A), [Fe^{2+}] (mM), and [CPG] (mM)) with the output parameter ([CPG] removal (%)). The experimental design is reported in Table 1, where the most favorable experimental values are highlighted in bold and underlined.

Table 1. Doehlert matrix experiments and results for CPG removal by the electro-Fenton process.

Experiment Number	Coded Variables			Real Variables			Results
	X_1	X_2	X_3	Current Intensity:	Fe^{2+} Concentration:	CPG Concentration:	Y (%)
				U_1 (A)	U_2 (mM)	U_3 (mM)	
1	1	0	0	0.55	0.6	0.06	88.9
2	−1	0	0	0.05	0.6	0.06	24.9
3	$\frac{1}{2}$	$\frac{\sqrt{3}}{2}$	0	0.42	1.0	0.06	75.5
4	$-\frac{1}{2}$	$-\frac{\sqrt{3}}{2}$	0	0.17	0.2	0.06	42.0
5	$\frac{1}{2}$	$-\frac{\sqrt{3}}{2}$	0	0.42	0.2	0.06	66.5
6	$-\frac{1}{2}$	$\frac{\sqrt{3}}{2}$	0	0.17	1.0	0.06	45.1
7	$\frac{1}{2}$	$\frac{\sqrt{3}}{6}$	$\frac{\sqrt{6}}{3}$	0.42	0.7	0.10	60.9
8	$-\frac{1}{2}$	$-\frac{\sqrt{3}}{6}$	$-\frac{\sqrt{6}}{3}$	0.17	0.5	0.02	62.4
9	$\frac{1}{2}$	$-\frac{\sqrt{3}}{6}$	$-\frac{\sqrt{6}}{3}$	0.42	0.5	0.02	81.6
10	0	$\frac{\sqrt{3}}{3}$	$-\frac{\sqrt{6}}{3}$	0.30	0.9	0.02	72.1
11	$-\frac{1}{2}$	$\frac{\sqrt{3}}{6}$	$\frac{\sqrt{6}}{3}$	0.17	0.7	0.10	38.0
12	0	$-\frac{\sqrt{3}}{3}$	$\frac{\sqrt{6}}{3}$	0.30	0.3	0.10	57.6
13	0	0	0	0.30	0.6	0.06	68.5
14	0	0	0	0.30	0.6	0.06	68.5
15	0	0	0	0.30	0.6	0.06	68.5

Equation (7) embodies the complex interplay among the three independent variables by incorporating their interaction terms and quadratic effects.

$$Y = 68.5 + 30.5\ X_1 + 1.5\ X_2 - 12.2\ X_3 + 3.4\ X_1X_2 + 1.1\ X_1X_3 - 5.7\ X_2X_3 - 11.6\ X_1^2 - 11.1\ X_2^2 - 3.9\ X_3^2 \quad (7)$$

Following statistical analysis, parameters with a probability lower than 0.05, indicating significant explanatory power, were identified and marked with an asterisk (*) in Table 2. Conversely, parameters with a probability greater than 0.05, indicating a lack of statistically significant influence, were excluded from the model for parsimony. The resulting equation (Equation (8)) representing the model is shown below:

$$Y = 68.5 + 30.5\ X_1 - 12.2\ X_3 - 11.6\ X_1^2 - 11.1\ X_2^2 \quad (8)$$

Table 2. Statistical data of the Doehlert model.

i	Term	b_i	Std Error	t Ratio	Prob > |t|
0	Constant	68.5	2.300475	29.78	<0.0001
1	X_1	30.5	2.300475	13.25	0.0002
2	X_2	1.5	1.992271	0.73	0.5049
3	X_3	−12.2	1.992261	−6.11	0.0036
4	X_1X_2	3.4	4.601085	0.74	0.5002
5	X_1X_3	1.1	5.144056	0.21	0.8466
6	X_2X_3	−5.7	5.143613	−1.10	0.3331
7	X_1X_1	−11.6	3.63737	−3.19	0.0332
8	X_2X_2	−11.1	3.637584	−3.05	0.0380
9	X_3X_3	−3.9	3.450617	−1.14	0.3189

The exclusion of statistically insignificant terms resulted in a reduction in model complexity, as evidenced by the simpler resulting equation (Equation (8)). This later result, along with the results presented in Figure 1, indicates moderately positive correlations within the model.

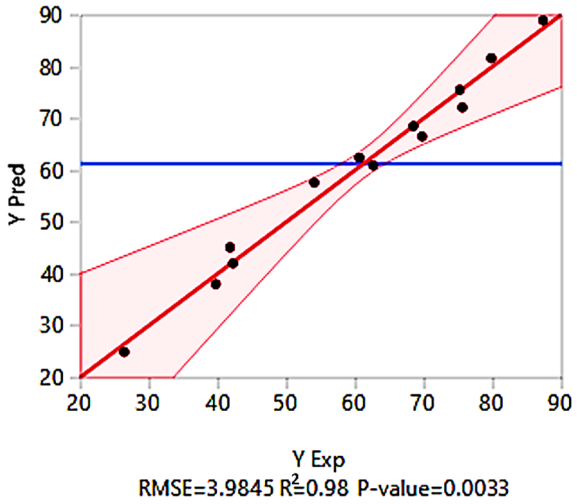

Figure 1. Correlation between experimental values and the Doehlert model predictions for CPG removal by the electro-Fenton process. The red line represents the fitted linear regression line, the red bands represent the confidence interval bands, and the blue line represents the horizontal null model line.

The *p*-value is confirmed to be strictly below 0.05, statistically affirming the significance of the model. Moreover, the observation of a high F-ratio in conjunction with a low *p*-value provides statistical evidence for the significance of the equation. This implies that the model effectively captures relationships among the variables beyond random variation.

Table 2 provides essential statistical data crucial for the development and comprehension of the Doehlert model. Additionally, it displays the performance of the Doehlert model by presenting various error metrics.

3.2. Response Surface Analysis

CPG degradation is illustrated in Figure 2 with the isoresponse curves and their corresponding three-dimensional representations. According to these graphs, raising the current intensity from 0.05 to 0.55 A upgraded the CPG removal rate from 29.7 to 83.2% for 15 min reaction time, proving the increase in decomposition efficiency (Figure 2a,b).

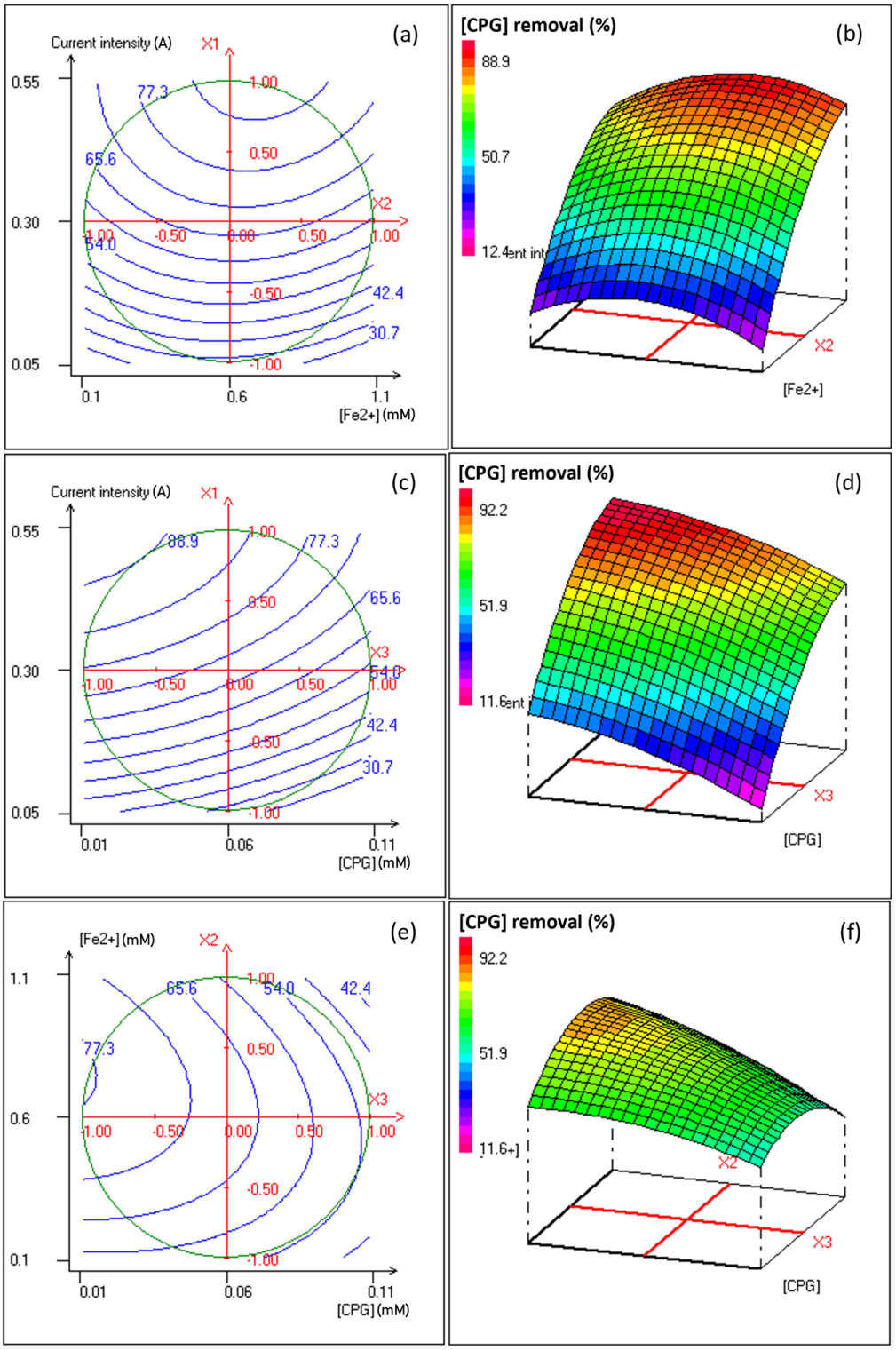

Figure 2. (**a**) Isoresponse curves of CPG removal versus current intensity (A) and the initial Fe^{2+} concentration (mM); (**b**) corresponding 3D surface plot; (**c**) Isoresponse curves of CPG removal versus current intensity (A) and the initial CPG concentration (mM); (**d**) corresponding 3D surface plot; (**e**) Isoresponse curves of CPG removal versus the initial Fe^{2+} concentration (mM) and the initial CPG concentration (mM); and (**f**) corresponding 3D surface plot. The results were obtained from the Doehlert matrix (Table 2). The experimental conditions were $[Na_2SO_4]$ = 50 mM, pH = 3, t = 15 min, and V = 0.3 L. The blue curves represent the isoresponse curves and the green circle represents the studied domain.

The enhanced CPG removal rate results from the combined effect of excess H_2O_2 production and efficient Fe^{2+} regeneration at the cathode (Equation (9)), which directly leads to an increase in hydroxyl radical production (Equation (10)) and therefore improves the efficiency of treatment [29,49]. These results align with those reported by Dirany et al. [50] in their investigation of operating parameters for the electro-Fenton treatment of water contaminated with sulfamethoxazole. Oturan et al. [51] reported similar results for the treatment of phenylurea herbicides. In addition, Özcan et al. [52] reported that a high current intensity decreases the degradation rate and attributed this behavior to the $4e^-$ reduction of O_2 (Equation (11)), which favors the production of H_2O, thereby competing with and inhibiting the reaction that generates H_2O_2 (Equation (12)).

$$Fe^{3+} + e^- \rightarrow Fe^{2+} \quad (9)$$

$$Fe^{2+} + H_2O_2 \rightarrow Fe^{3+} + OH^- + {}^{\bullet}OH \quad \text{(Fenton's reaction)} \quad (10)$$

$$O_2 + 4e^- + 4H^+ \rightarrow 2H_2O \quad (11)$$

$$O_2 + 2e^- + 2H^+ \rightarrow H_2O_2 \quad (12)$$

Moreover, according to Figure 2c,d, the CPG removal rate exhibited an inverse correlation with the initial CPG concentration, indicating that higher starting concentrations resulted in poorer removal. The removal rate decreased from 88.9 to 30.7% as the $[CPG]_0$ increased from 0.02 to 0.1 mM, respectively. The observed behavior can be attributed to competition for hydroxyl radicals. At high initial CPG concentrations, the generated intermediates preferentially consume these radicals, hindering the degradation of the target pollutant.

Indeed, as the CPG concentration increases, the ratio of CPG molecules to hydroxyl radicals becomes unfavorable for efficient removal. The hydroxyl radicals are rapidly depleted, limiting degradation [36].

Furthermore, an increase in the initial Fe^{2+} concentration enhanced the treatment's effectiveness. Indeed, the CPG degradation improved when the initial concentration of ferrous ions rose from 0.2 to 0.7 mM (Figure 2e,f). This behavior is explained by the higher concentration of Fe^{2+} ions in the reaction mixture that promotes a more efficient generation of ${}^{\bullet}OH$, which is the potent oxidizer driving the degradation process [53]. However, a high initial ferrous ion concentration ($[Fe^{2+}]_0 > 0.7$ mM) resulted in a decrease in the degradation rate, indicating that the excess of Fe^{2+} exhibits scavenging behavior through its consumption of the ${}^{\bullet}OH$ (Equation (13)) [53,54]. This behavior diminished the amount of ${}^{\bullet}OH$ and ultimately reduced the rate of the degradation reaction. Tran et al. [55] reported similar results for the degradation of a glyphosate herbicide by an electro-Fenton process using a carbon felt cathode.

$$Fe^{2+} + {}^{\bullet}OH \rightarrow Fe^{3+} + OH^- \quad (13)$$

3.3. Improved Grey Wolf Optimization

The improved grey wolf optimizer was employed to optimize CPG removal conditions. This optimization method was selected for its ability to explore the solution space efficiently, ensuring a thorough search for potential solutions. Additionally, it demonstrates a strong convergence capability, reliably reaching high-quality results. The IGWO algorithm was configured to optimize the parameters of the Doehlert model, with the objective of identifying key factors influencing CPG degradation performance.

Following the initial configuration, IGWO proceeded through numerous iterations. In each iteration, the algorithm adjusted the experimental conditions based on the performance of the previous cycle. This iterative process aimed to maximize the specified performance criterion, which, in this case, was achieving the best possible CPG degradation. Upon convergence of IGWO towards promising solutions, the identified optimal conditions for CPG degradation were documented in a tabular format (Figure 3).

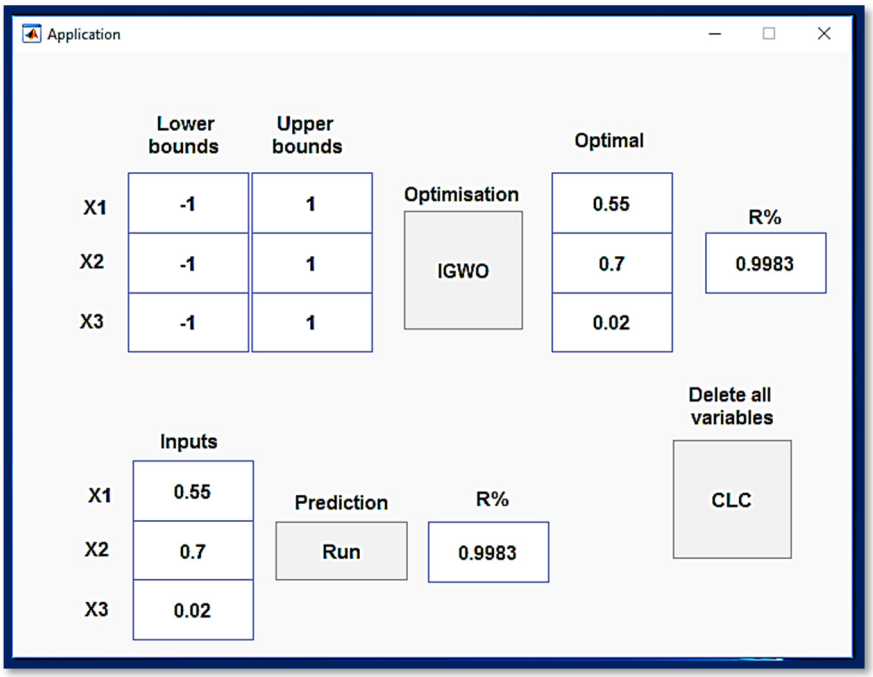

Figure 3. Optimization of CPG removal by the electro−Fenton process using IGWO. X1: current intensity (mA), X2: Fe^{2+} initial concentration (mM), X3: CPG initial concentration (mM), R%: [CPG] removal rate (%).

In order to facilitate user interaction with the IGWO algorithm, a novel Matlab-based interface was developed. This application streamlines the optimization workflow by offering a user-friendly platform for configuring IGWO parameters, running the optimization algorithm, and visualizing the results. Through this interface, researchers can easily analyze the results, track the optimization process, and interactively explore the solution space.

Based on the data reported in Figure 3, the optimal operating conditions for the removal of CPG (0.02 mM) correspond to a current intensity of 0.55 A, an initial concentration of 0.7 mM in ferrous ions, and an initial concentration of 0.02 mM in clopidogrel. Under these optimized conditions, the predicted degradation rate of CPG is estimated to be 99.83%. These findings underscore the efficacy of the IGWO algorithm in identifying parameter configurations that maximize the efficiency of CPG degradation.

3.4. Validation of Optimal Conditions

In order to confirm the reliability and applicability of the Doehlert model's predictions and the efficacy of the resulting optimal conditions, a laboratory-based validation phase was conducted. CPG degradation was examined during the electro-Fenton reaction, with removal rate measurements taken at defined intervals. This implemented monitoring strategy facilitated the achievement of the following two key objectives: confirmation of treatment effectiveness and determination of degradation kinetic. The analysis of the obtained results reveals the total disappearance of CPG after 20 min of reaction time (Figure 4), confirming the initial prediction of the Doehlert model. This strong concordance between the model's predictions and the experimental data provides compelling evidence for the validity and robustness of the overall methodological approach.

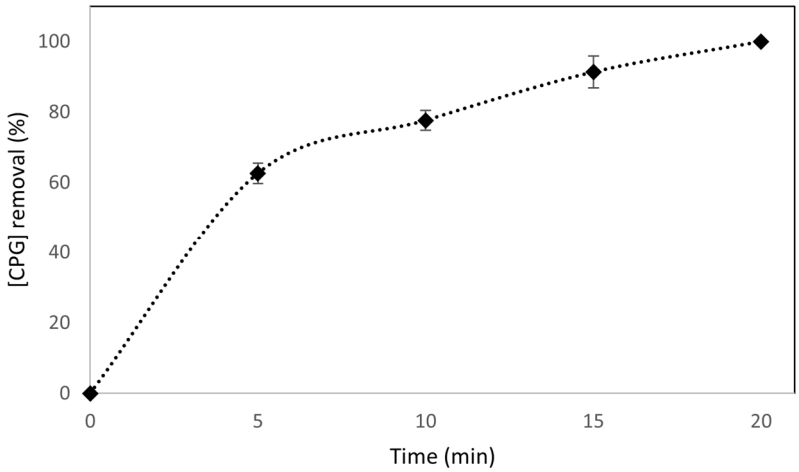

Figure 4. Time evolution of CPG removal during the electro-Fenton treatment. The experimental conditions were $[CPG]_0$ = 0.02 mM, $[Fe^{2+}]$ = 0.7 mM, $[Na_2SO_4]$ = 50 mM, pH = 3, I = 0.55 A, t = 20 min, and V = 0.3 L.

3.5. Mineralization of Clopidogrel

The application of the optimal operating conditions, as deduced from the Doehlert matrix design, resulted in the complete elimination of CPG within the synthetic effluent. Contrarily, the mineralization rate stayed low throughout the experiment, reaching only 36% after 120 min of reaction time from a starting concentration of 3.84 mg L^{-1} O_2 (Figure 5). The generation of persistent organic by-products during the treatment is a possible explanation for the low mineralization rate. These by-products may interfere with the complete degradation of the target pollutant. Indeed, the disappearance of CPG was pursued by the subsequent appearance of intermediate compounds, leading to the competitive consumption of hydroxyl radicals. This finding was confirmed by the observed rapid destruction of CPG and the limited decrease in TOC [56]. Furthermore, extending the reaction time from 120 to 480 min upgraded the TOC removal rate from 36 to 70.4%, proving that the mineralization yield increased over time.

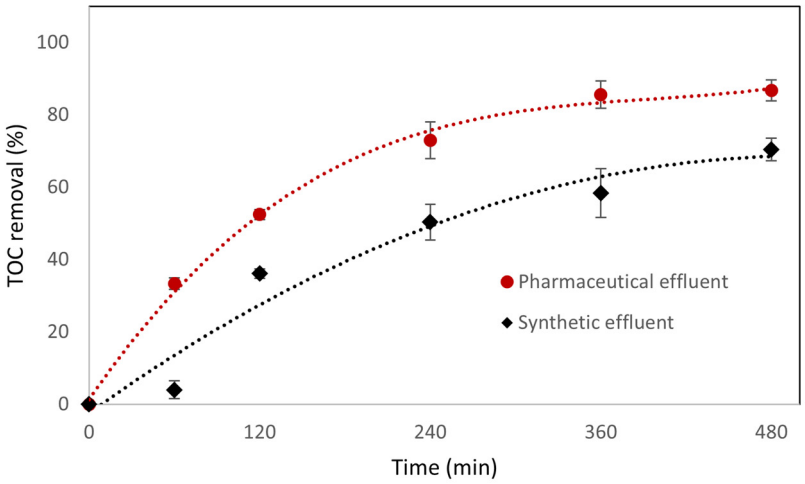

Figure 5. Time evolution of TOC removal during the electro−Fenton treatment. The experimental conditions were $[CPG]_0$ = 0.02 mM, $[Fe^{2+}]$ = 0.7 mM, $[Na_2SO_4]$ = 50 mM, pH = 3, I = 0.55 A, t = 8 h, and V = 0.3 L.

3.6. Application to Real Industrial Wastewater

The studied pharmaceutical effluent was analyzed and examined following the protocols indicated in Section 2.3. An overview of the effluent's key characteristics is provided in Table 3.

Table 3. Main characteristics of the real industrial pharmaceutical effluent.

	Pharmaceutical Effluent
pH	6
Conductivity (μS cm^{-1})	343
TSS (mg L^{-1})	152
TDS (mg L^{-1})	204.4
COD (mg L^{-1})	1650
TOC (mg L^{-1})	498
TN_b (mg L^{-1})	83.9
[CPG] (mg L^{-1})	181.5
[NO_3^-] (mg L^{-1})	49.1
[NO_2^-] (mg L^{-1})	0.23
[PO_4^{3-}] (mg L^{-1})	31

The result examination identified a high level of CPG contamination in the analyzed real wastewater sample (181.5 mg·L^{-1}). Additionally, it had an initial COD of 1650 mg·L^{-1}, with a TOC of 498 mg·L^{-1} (Table 3).

The mineralization process for the industrial effluent was conducted under the same operating conditions as the synthetic effluent. According to Figure 5, the TOC removal rate increased at the beginning of the reaction significantly; it reached 73% after 240 min of electrolysis time. Beyond this first phase, the evolution of the mineralization became considerably slower, and the TOC decreased slightly over time to achieve, at the end of treatment, a rate of 87%. Indeed, the degradation of CPG generates aromatic intermediates that undergo oxidation themselves, leading to the opening of the aromatic cycle and the appearance of recalcitrant organic compounds like short-chain aliphatic carboxylic acids. Aromatic cycles are more susceptible to attacks by $^{\bullet}$OH than aliphatic compounds, which exhibit greater resistance and are therefore difficult to oxidize [45,57]. In addition, this behavior may be a consequence of Fe(III) complexation with carboxylic acids, where the latter decrease the efficiency of mineralization significantly compared with the rate observed at the beginning of treatment because of their stability and low reactivity toward hydroxyl radicals [58]. Furthermore, an evaluation of the system's energy consumption was conducted through careful calculations based on Equation (1), which was found to be 1.4 kWh·kg^{-1} $TOC_{removed}$.

4. Conclusions

The performance of the electro-Fenton process in removing the antiplatelet drug clopidogrel from wastewater was investigated. The Doehlert design was employed to examine the influence of various experimental parameters (initial Fe^{2+} concentration, current intensity, and initial CPG concentration) and their interaction. In addition, the quadratic polynomial model demonstrated good performance and was deemed suitable for predicting within the investigated studied domain. The improved grey wolf optimizer was employed to demonstrate its relevance in optimizing the electro-Fenton process. According to the obtained results, total CPG disappearance was achieved after 20 min of reaction time, at a current intensity of 0.55 A, for an initial CPG concentration of 0.02 mM and an initial Fe^{2+} concentration of 0.7 mM. The aforementioned conditions were subsequently

implemented in the mineralization stage, leading to a TOC removal rate of 70.4% after 480 min of electrolysis time, which indicates the generation of persistent intermediates. Furthermore, the treatment of a real pharmaceutical effluent using the electro-Fenton process at optimal conditions resulted in an impressive 87% mineralization efficiency after 480 min of reaction time.

Author Contributions: Conceptualization, D.M., H.T. and A.A.; data curation, D.M.; formal analysis, D.M., E.A. and J.H.; investigation, S.T., S.M., N.B. and A.A.; methodology, D.M., E.A., H.T. and A.A.; resources, A.K.D.A., M.S. and A.A.; software, D.M. and H.T.; supervision, H.B. and A.A.; validation, D.M.; visualization, A.A.; writing—original draft, D.M. and H.T.; writing—review and editing, H.B. and A.A. All authors have read and agreed to the published version of the manuscript.

Funding: This research was funded by the Scientific Research Deanship at the University of Hail, Saudi Arabia, through project number RG–21 171.

Data Availability Statement: The data that support the findings of this study are available from the corresponding author upon reasonable request.

Acknowledgments: The authors express their sincere thanks to the University of Hail, Kingdom of Saudi Arabia, for financing this study. Thanks go also to the Chemistry Department in the College of Sciences at Hail University for their valuable assistance in providing the required information.

Conflicts of Interest: The authors declare that they have no known competing financial interests or personal relationships that could appear to influence the work reported in this paper.

References

1. Karungamye, P.; Rugaika, A.; Mtei, K.; Machunda, R. The Pharmaceutical Disposal Practices and Environmental Contamination: A Review in East African Countries. *HydroResearch* **2022**, *5*, 99–107. [CrossRef]
2. Jones, O.A.H.; Voulvoulis, N.; Lester, J.N. Human Pharmaceuticals in Wastewater Treatment Processes. *Crit. Rev. Environ. Sci. Technol.* **2005**, *35*, 401–427. [CrossRef]
3. Ajiboye, T.O.; Oladoye, P.O.; Omotola, E.O. Adsorptive Reclamation of Pharmaceuticals from Wastewater Using Carbon-Based Materials: A Review. *Kuwait J. Sci.* **2024**, *51*, 100225. [CrossRef]
4. Roslan, N.N.; Lau, H.L.H.; Suhaimi, N.A.A.; Shahri, N.N.M.; Verinda, S.B.; Nur, M.; Lim, J.-W.; Usman, A. Recent Advances in Advanced Oxidation Processes for Degrading Pharmaceuticals in Wastewater—A Review. *Catalysts* **2024**, *14*, 189. [CrossRef]
5. Sacco, N.A.; Marchesini, F.A.; Gamba, I.; García, G. Photoelectrochemical Degradation of Contaminants of Emerging Concern with Special Attention on the Removal of Acetaminophen in Water-Based Solutions. *Catalysts* **2023**, *13*, 524. [CrossRef]
6. Imparato, C.; Bifulco, A.; Silvestri, B.; Vitiello, G. Recent Advances in Endocrine Disrupting Compounds Degradation through Metal Oxide-Based Nanomaterials. *Catalysts* **2022**, *12*, 289. [CrossRef]
7. Dharmaraj, S.; Ashokkumar, V.; Pandiyan, R.; Halimatul Munawaroh, H.S.; Chew, K.W.; Chen, W.-H.; Ngamcharussrivichai, C. Pyrolysis: An Effective Technique for Degradation of COVID-19 Medical Wastes. *Chemosphere* **2021**, *275*, 130092. [CrossRef]
8. Adeoye, J.B.; Tan, Y.H.; Lau, S.Y.; Tan, Y.Y.; Chiong, T.; Mubarak, N.M.; Khalid, M. Advanced Oxidation and Biological Integrated Processes for Pharmaceutical Wastewater Treatment: A Review. *J. Environ. Manag.* **2024**, *353*, 120170. [CrossRef]
9. Fallah, Z.; Zare, E.N.; Ghomi, M.; Ahmadijokani, F.; Amini, M.; Tajbakhsh, M.; Arjmand, M.; Sharma, G.; Ali, H.; Ahmad, A.; et al. Toxicity and Remediation of Pharmaceuticals and Pesticides Using Metal Oxides and Carbon Nanomaterials. *Chemosphere* **2021**, *275*, 130055. [CrossRef]
10. Omotola, E.O.; Genthe, B.; Ndlela, L.; Olatunji, O.S. Environmental Risk Characterization of an Antiretroviral (ARV) Lamivudine in Ecosystems. *Int. J. Environ. Res. Public Health* **2021**, *18*, 8358. [CrossRef]
11. Parida, V.K.; Sikarwar, D.; Majumder, A.; Gupta, A.K. An Assessment of Hospital Wastewater and Biomedical Waste Generation, Existing Legislations, Risk Assessment, Treatment Processes, and Scenario during COVID-19. *J. Environ. Manag.* **2022**, *308*, 114609. [CrossRef]
12. Sathishkumar, P.; Meena, R.A.A.; Palanisami, T.; Ashokkumar, V.; Palvannan, T.; Gu, F.L. Occurrence, Interactive Effects and Ecological Risk of Diclofenac in Environmental Compartments and Biota—A Review. *Sci. Total Environ.* **2020**, *698*, 134057. [CrossRef]
13. Vumazonke, S.; Khamanga, S.M.; Ngqwala, N.P. Detection of Pharmaceutical Residues in Surface Waters of the Eastern Cape Province. *Int. J. Environ. Res. Public Health* **2020**, *17*, 4067. [CrossRef]
14. De Ilurdoz, M.S.; Sadhwani, J.J.; Reboso, J.V. Antibiotic Removal Processes from Water & Wastewater for the Protection of the Aquatic Environment—A Review. *J. Water Process Eng.* **2022**, *45*, 102474. [CrossRef]
15. Oad, N.; Chandra, P.; Mohammad, A.; Tripathi, B.; Yoon, T. MoS2-Based Hetero-Nanostructures for Photocatalytic, Photoelectrocatalytic and Piezocatalytic Remediation of Hazardous Pharmaceuticals. *J. Environ. Chem. Eng.* **2023**, *11*, 109604. [CrossRef]

16. Park, J.; Kim, C.; Hong, Y.; Lee, W.; Chung, H.; Jeong, D.-H.; Kim, H. Distribution and Removal of Pharmaceuticals in Liquid and Solid Phases in the Unit Processes of Sewage Treatment Plants. *Int. J. Environ. Res. Public Health* **2020**, *17*, 687. [CrossRef] [PubMed]
17. Son, D.-J.; Kim, C.-S.; Lee, J.-H.; Yoon, J.-K.; Lee, S.-H.; Jeong, D.-H. Occurrence Assessment of Pharmaceuticals in Various Sewage Treatment Plants and Effluent-Receiving Streams in Korea. *Water* **2023**, *15*, 3897. [CrossRef]
18. De Melo Franco Domingos, J.; De Alencar Neves, T.; De Sousa Maia, D.L.; Carvalho Siqueira, R.; Araújo Marques, M.V.; Alves, O.L.; Guimarães, J.R.; Antunes Nolasco, M.; Rosa, A.H. Effect of the Association of Coagulation/Flocculation, Hydrodynamic Cavitation, Ozonation and Activated Carbon in Landfill Leachate Treatment System. *Sci. Rep.* **2023**, *13*, 9502. [CrossRef]
19. Suleiman, M.; Demaria, F.; Zimmardi, C.; Kolvenbach, B.A.; Corvini, P.F.-X. Analyzing Microbial Communities and Their Biodegradation of Multiple Pharmaceuticals in Membrane Bioreactors. *Appl. Microbiol. Biotechnol.* **2023**, *107*, 5545–5554. [CrossRef]
20. Ilavský, J.; Barloková, D. The Removal of Selected Pharmaceuticals from Water by Adsorption with Granular Activated Carbons. In Proceedings of the 4th International Conference on Advances in Environmental Engineering, Ostrava, Czech Republic, 20–22 November 2023; p. 33.
21. Esteki, S.; Karsaz, M.; Ghofrani, B.; Yegani, R.; Majidi, S. Combination of Membrane Bioreactor with Chemical Coagulation for the Treatment of Real Pharmaceutical Wastewater: Comparison of Simultaneous and Consecutive Pre-Treatment of Coagulation on MBR Performance. *J. Water Process Eng.* **2024**, *60*, 105108. [CrossRef]
22. Mansour, D.; El-Sofany, W.I.; Abdella, F.I.A.; Masood, N.; Khalaf Dhahi Alsukaibi, A.; Bellakhal, N. Doehlert Experimental Design for the Optimization of Electrocoagulation Treatment of Landfill Leachate. *Environ. Pollut. Bioavailab.* **2021**, *33*, 395–401. [CrossRef]
23. Jiad, M.M.; Abbar, A.H. Treatment of Petroleum Refinery Wastewater by Electrofenton Process Using a Low Cost Porous Graphite Air-Diffusion Cathode with a Novel Design. *Chem. Eng. Res. Des.* **2023**, *193*, 207–221. [CrossRef]
24. Oturan, M.A.; Aaron, J.-J. Advanced Oxidation Processes in Water/Wastewater Treatment: Principles and Applications. A Review. *Crit. Rev. Environ. Sci. Technol.* **2014**, *44*, 2577–2641. [CrossRef]
25. Akpotu, S.O.; Oseghe, E.O.; Ayanda, O.S.; Skelton, A.A.; Msagati, T.A.M.; Ofomaja, A.E. Photocatalysis and Biodegradation of Pharmaceuticals in Wastewater: Effect of Abiotic and Biotic Factors. *Clean Technol. Environ. Policy* **2019**, *21*, 1701–1721. [CrossRef]
26. Liu, Z.; Wardenier, N.; Hosseinzadeh, S.; Verheust, Y.; De Buyck, P.-J.; Chys, M.; Nikiforov, A.; Leys, C.; Van Hulle, S. Degradation of Bisphenol A by Combining Ozone with UV and H_2O_2 in Aqueous Solutions: Mechanism and Optimization. *Clean Technol. Environ. Policy* **2018**, *20*, 2109–2118. [CrossRef]
27. Rashmishree, K.N.; Bhaskar, S.; Shri Hari, S.; Thalla, A.K. Correction: Green Synthesis of Laterite Iron-based Nanocatalysts Using Psidium Guajava and Macaranga Peltata Plant Extract for Its Catalytic Application in Fenton's Oxidation of Triclosan. *Clean Technol. Environ. Policy* **2023**, *25*. [CrossRef]
28. Gasmi, I.; Hamdaoui, O.; Ferkous, H.; Alghyamah, A. Sonochemical Advanced Oxidation Process for the Degradation of Furosemide in Water: Effects of Sonication's Conditions and Scavengers. *Ultrason. Sonochem.* **2023**, *95*, 106361. [CrossRef] [PubMed]
29. Mansour, D.; Fourcade, F.; Soutrel, I.; Hauchard, D.; Bellakhal, N.; Amrane, A. Mineralization of Synthetic and Industrial Pharmaceutical Effluent Containing Trimethoprim by Combining Electro-Fenton and Activated Sludge Treatment. *J. Taiwan Inst. Chem. Eng.* **2015**, *53*, 58–67. [CrossRef]
30. Al Marzouqi, F.; Selvaraj, R. Surface Plasmon Resonance Induced Photocatalysis in 2D/2D Graphene/g-C_3N_4 Heterostructure for Enhanced Degradation of Amine-Based Pharmaceuticals under Solar Light Illumination. *Catalysts* **2023**, *13*, 560. [CrossRef]
31. Mansour, D.; Fourcade, F.; Huguet, S.; Soutrel, I.; Bellakhal, N.; Dachraoui, M.; Hauchard, D.; Amrane, A. Improvement of the Activated Sludge Treatment by Its Combination with Electro Fenton for the Mineralization of Sulfamethazine. *Int. Biodeterior. Biodegrad.* **2014**, *88*, 29–36. [CrossRef]
32. Puga, A.; Moreira, M.M.; Figueiredo, S.A.; Delerue-Matos, C.; Pazos, M.; Rosales, E.; Sanromán, M.Á. Electro-Fenton Degradation of a Ternary Pharmaceutical Mixture and Its Application in the Regeneration of Spent Biochar. *J. Electroanal. Chem.* **2021**, *886*, 115135. [CrossRef]
33. Mahmoudi, N.; Farhadian, M.; Solaimany Nazar, A.R.; Eskandari, P.; Esfahani, K.N. Investigation and Optimization of the Performance of Sono-Photo-Electro-Fenton Process for Removal of Acid Black 172 and Disperse Blue 56 from Polluted Water: Comparison of the Degradation Activity with Electro-Fenton-Based Processes. *Int. J. Environ. Sci. Technol.* **2022**, *19*, 1671–1682. [CrossRef]
34. Sobczak, M.; Bujnowicz, S.; Bilińska, L. Fenton and Electro-Fenton Treatment for Industrial Textile Wastewater Recycling. Comparison of by-Products Removal, Biodegradability, Toxicity, and Re-Dyeing. *Water Resour. Ind.* **2024**, *31*, 100256. [CrossRef]
35. El Jery, A.; Aldrdery, M.; Shirode, U.R.; Gavilán, J.C.O.; Elkhaleefa, A.; Sillanpää, M.; Sammen, S.S.; Tizkam, H.H. An Efficient Investigation and Machine Learning-Based Prediction of Decolorization of Wastewater by Using Zeolite Catalyst in Electro-Fenton Reaction. *Catalysts* **2023**, *13*, 1085. [CrossRef]
36. Mansour, D.; Fourcade, F.; Bellakhal, N.; Dachraoui, M.; Hauchard, D.; Amrane, A. Biodegradability Improvement of Sulfamethazine Solutions by Means of an Electro-Fenton Process. *Water Air Soil Pollut.* **2012**, *223*, 2023–2034. [CrossRef]

37. Mansour, D.; Fourcade, F.; Soutrel, I.; Hauchard, D.; Bellakhal, N.; Amrane, A. Relevance of a Combined Process Coupling Electro-Fenton and Biological Treatment for the Remediation of Sulfamethazine Solutions—Application to an Industrial Pharmaceutical Effluent. *Comptes Rendus Chim.* **2015**, *18*, 39–44. [CrossRef]
38. Chi, C.; Zhou, X.; Wang, Y.; Gao, X.; Bai, J.; Guo, Y.; Ni, J. Treatment of Coking Wastewater Using a Needle Coke Electro-Fenton Cathode: Optimizing of COD, NH_4+-N, and TOC Removal and Characterization of Pollutants. *Water Sci. Technol.* **2023**, *88*, 106–122. [CrossRef]
39. Oturan, M.A. Outstanding Performances of the BDD Film Anode in Electro-Fenton Process: Applications and Comparative Performance. *Curr. Opin. Solid State Mater. Sci.* **2021**, *25*, 100925. [CrossRef]
40. García-Espinoza, J.D.; Robles, I.; Durán-Moreno, A.; Godínez, L.A. Study of Simultaneous Electro-Fenton and Adsorption Processes in a Reactor Containing Porous Carbon Electrodes and Particulate Activated Carbon. *J. Electroanal. Chem.* **2021**, *895*, 115476. [CrossRef]
41. Al-Shomar, S.M.; Mansour, D.; Hedhili, F.; Aslam, A.; Mahmoud, S.A.; Akl, A.A.; Shaaban, E.R. Photocatalytic Treatment of Industrial Effluent Containing Clopidogrel Using Europium Doped TiO_2 Thin Films under Solar Irradiation. *React. Kinet. Mech. Catal.* **2022**, *135*, 2813–2825. [CrossRef]
42. Fedeila, M.; Hachaïchi-Sadouk, Z.; Bautista, L.F.; Simarro, R. Biodegradation of Clopidogrel Bisulfate by Pseudomonas Aeruginosa and Pseudomonas Putida Strains Isolated from Algerian Wastewater. *J. Contam. Hydrol.* **2023**, *256*, 104198. [CrossRef]
43. El Faroudi, L.; El Jemli, Y.; Zari, R.; Barakat, A.; Ismael, M.K.; Abdelouahdi, K.; Solhy, A. Optimization of Photocatalytic Parameters Using Doehlert Experimental Design to Improve the Photodegradation of Orange G. *J. Photochem. Photobiol. A Chem.* **2023**, *445*, 115012. [CrossRef]
44. Ben Khalifa, E.; Cecone, C.; Rzig, B.; Azaiez, S.; Cesano, F.; Malandrino, M.; Bracco, P.; Magnacca, G. Green Surface Modification of Polyvinyl Alcohol Fibers and Its Application for Dye Removal Using Doehlert Experimental Design. *React. Funct. Polym.* **2023**, *193*, 105763. [CrossRef]
45. Mansour, D.; Alblawi, E.; Alsukaibi, A.K.D.; Al Shammari, B. Removal of Congo Red Dye by Electrochemical Advanced Oxidation Process: Optimization, Degradation Pathways, and Mineralization. *Sustain. Water Resour. Manag.* **2024**, *10*, 41. [CrossRef]
46. Hammami, S.; Ouejhani, A.; Bellakhal, N.; Dachraoui, M. Application of Doehlert Matrix to Determine the Optimal Conditions of Electrochemical Treatment of Tannery Effluents. *J. Hazard. Mater.* **2009**, *163*, 251–258. [CrossRef]
47. Mathieu, D.; Nony, J.; Phan-Tan-Luu, R. *New Efficient Methodology for Research Using Optimal Design (NEMRODW) Software*; LPRAI, University Aix-Marseille III: Marseille, France, 2000.
48. Nadimi-Shahraki, M.H.; Taghian, S.; Mirjalili, S. An Improved Grey Wolf Optimizer for Solving Engineering Problems. *Expert Syst. Appl.* **2021**, *166*, 113917. [CrossRef]
49. Atmaca, E. Treatment of Landfill Leachate by Using Electro-Fenton Method. *J. Hazard. Mater.* **2009**, *163*, 109–114. [CrossRef]
50. Dirany, A.; Sirés, I.; Oturan, N.; Oturan, M.A. Electrochemical Abatement of the Antibiotic Sulfamethoxazole from Water. *Chemosphere* **2010**, *81*, 594–602. [CrossRef]
51. Oturan, M.A.; Edelahi, M.C.; Oturan, N.; El Kacemi, K.; Aaron, J.-J. Kinetics of Oxidative Degradation/Mineralization Pathways of the Phenylurea Herbicides Diuron, Monuron and Fenuron in Water during Application of the Electro-Fenton Process. *Appl. Catal. B Environ.* **2010**, *97*, 82–89. [CrossRef]
52. Özcan, A.; Şahin, Y.; Koparal, A.S.; Oturan, M.A. Degradation of Picloram by the Electro-Fenton Process. *J. Hazard. Mater.* **2008**, *153*, 718–727. [CrossRef]
53. Panizza, M.; Cerisola, G. Electro-Fenton Degradation of Synthetic Dyes. *Water Res.* **2009**, *43*, 339–344. [CrossRef] [PubMed]
54. Brillas, E.; Sirés, I.; Oturan, M.A. Electro-Fenton Process and Related Electrochemical Technologies Based on Fenton's Reaction Chemistry. *Chem. Rev.* **2009**, *109*, 6570–6631. [CrossRef] [PubMed]
55. Tran, M.H.; Nguyen, H.C.; Le, T.S.; Dang, V.A.D.; Cao, T.H.; Le, C.K.; Dang, T.-D. Degradation of Glyphosate Herbicide by an Electro-Fenton Process Using Carbon Felt Cathode. *Environ. Technol.* **2021**, *42*, 1155–1164. [CrossRef] [PubMed]
56. Hammami, S.; Bellakhal, N.; Oturan, N.; Oturan, M.A.; Dachraoui, M. Degradation of Acid Orange 7 by Electrochemically Generated •OH Radicals in Acidic Aqueous Medium Using a Boron-Doped Diamond or Platinum Anode: A Mechanistic Study. *Chemosphere* **2008**, *73*, 678–684. [CrossRef] [PubMed]
57. Haidar, M.; Dirany, A.; Sirés, I.; Oturan, N.; Oturan, M.A. Electrochemical Degradation of the Antibiotic Sulfachloropyridazine by Hydroxyl Radicals Generated at a BDD Anode. *Chemosphere* **2013**, *91*, 1304–1309. [CrossRef]
58. Oturan, N.; Wu, J.; Zhang, H.; Sharma, V.K.; Oturan, M.A. Electrocatalytic Destruction of the Antibiotic Tetracycline in Aqueous Medium by Electrochemical Advanced Oxidation Processes: Effect of Electrode Materials. *Appl. Catal. B Environ.* **2013**, *140–141*, 92–97. [CrossRef]

Disclaimer/Publisher's Note: The statements, opinions and data contained in all publications are solely those of the individual author(s) and contributor(s) and not of MDPI and/or the editor(s). MDPI and/or the editor(s) disclaim responsibility for any injury to people or property resulting from any ideas, methods, instructions or products referred to in the content.